ASC'98 Palm Desert
September 14-18, 1998

Critical Current of Superconducting Rutherford Cable in High Magnetic Fields with Transverse Pressure

Daniel R. Dietderich and Ronald M. Scanlan,
Lawrence Berkeley National Laboratory, Berkeley, CA 94720

Robert P. Walsh and John R. Miller
National High Magnetic Field Laboratory, Tallahassee, FL 32706

Abstract—**For high energy physics applications superconducting cables are subjected to large stresses and high magnetic fields during service. It is essential to know how these cables perform in these operating conditions. A loading fixture capable of applying loads of up to 700kN has been developed by NHMFL for LBNL. This fixture permits uniform loading of straight cables over a 122 mm length in a split-pair solenoid in fields up to 12 T at 4.2 K. The first results from this system for Rutherford cables of internal-tin and modified jelly roll strand of Nb_3Sn produced by IGC and TWC showed that little permanent degradation occurs up to 210 MPa. However, the cable made from internal-tin strand showed a 40 % reduction in I_c at 11T and 210 MPa while a cable made from modified jelly roll material showed only a 15 % reduction in I_c at 11T and 185 MPa.**

I. Introduction

Large forces are produced when superconducting magnets are energized. Therefore, it is necessary to support the conductor to prevent large displacements that can strain the conductor beyond its elastic limit. These same forces also reduce the critical current of the conductor before the elastic limit is reached. To produce an optimum magnet design which best utilizes the superconductor material and maximizes the field the critical current variation with pressure is required.

For a cosine Θ magnet design large pressures are produced at the mid-plane of the magnet on the large face of the Rutherford cable. The magnets (i.e. common coil) presently being designed and built in the Superconducting Magnet Group (SMG) of Lawrence Berkeley National Laboratory such that the cable will be bi-axially loaded on both the face and the edge with the edge loading being about twice that applied to the face. Therefore information for loading in both orientations is required.

The results presented here are the first measurements performed at the National High Magnetic Field Laboratory (NHMFL) in a system designed for the SMG. These tests were performed on cable designed for and used in the inner coils of the world record dipole magnet D20 [1].

Manuscript received September 14, 1998.

This work was supported by the Director, Office of Energy Research, Office of High Energy and Nuclear Physics, High Energy Physics Division, U. S. Department of Energy, under Contract No. DE-AC03-6SF00098.

These cables were fabricated in our Group from modified jelly roll wire produced by Teledyne Wah Chang (TWC) and from internal tin wire manufactured by Intermagnetics General Corporation (IGC).

The results for both cables showed that very little if any permanent degradation occurred for transverse loads up to 185 to 210 MPa. However, the critical current of the cable with IGC strand was reduced by 40 % with a transverse pressure of 210 MPa at 11 T. The I_c of the cable with TWC strand was only reduced by 15 % at 11T and 185 MPa. The behavior of both cables with loading was also different. The TWC strand showed a quadratic behavior with increasing pressure while the IGC strand showed a linear behavior.

These results have important ramifications for high field magnet designs beyond the 13.5 T of D20. Not only must the strain level be controlled to prevent irreversible damage at these higher fields but the reduction in critical current due to the lower T_c and B_{c2} with high pressure must be controlled.

II. Materials and Test System

A. Strand and Cable Characteristics

Two strands made by two manufacturers were used in the Rutherford cables of this study. Cable 523 was made from IGC strand while cable 522 was made from TWC strand. Each cable was rectangular and contained 37 strands. The cabling parameters are listed in Table I.

Strand specifications are given in Table II. The two strands had very different internal geometries. The TWC strand had more Cu stabilizer and each of its 120 sub-elements had its own diffusion barrier. (Fig. 1(a)) The IGC strand had less Cu stabilizer and a diffusion barrier around all of its 19 sub-elements (Fig. 1(b)).

Both cables were heat treated at the same time and received the following schedule: 210 °C for 121 h, 340 °C for 60 h, and 660 °C for 259 h. For heat treatment the samples were sealed in a stainless steel retort that was continuously purged with flowing argon.

The data has not been corrected for self-field but due to the bifilar nature of the test arrangement the correction should be small.

TABLE I
CABLE CHARACTERISTICS

Cable No.	MFG.	Cable Comp(%)	Thickness (mm)	Width (mm)	Cable Pitch Length (mm)
522	TWC	84.1	1.356	14.45	90
523	IGC	84.1	1.369	14.45	90

TABLE II
STRAND CHARACTERISTICS

Cable No.	Strand Dia. (mm)	Cu to SC fraction	Sub-elements Dia. (μm)	No. Sub-elements
522	0.75	1.08	50-70	122
523	0.75	0.67	140-190	19

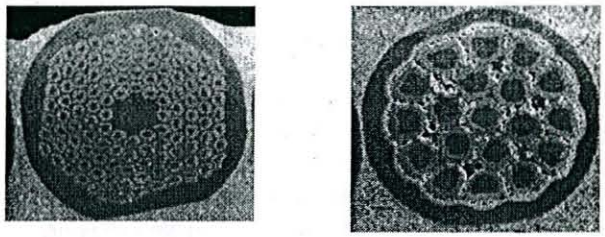

Fig. 1. (a) TWC strand of cable 522 and (b) IGC strand of cable 523 after heat treatment.

B. Cable Assembly

The cable stack in the loading region consisted of four cables, two active cables which carry the current and two dummies. The active cables carry the current in opposite directions and the dummy cables on either side of the active cables simulate a magnet environment and also reduce any stress concentration that may arise from non-uniform loading. For heat treatment the cable stack is placed into reaction tooling made of 304 stainless steel. The dimensions of the tooling and the shimming schedule were designed to confine as well as to compress the cable to its theoretical thickness, i.e. cable thickness plus insulation thickness. A sleeve of S-2 glass insulated each cable. The wall thickness of the sleeve was 0.125 mm. An additional sheet of S-2 glass with a thickness of 0.25 mm was wrapped around the cable stack without an overlap before putting it into the reaction tooling.

Three solder box connections were made to each sample. At the top of each sample the active cables are displaced from each other by a hard way bend forming a wishbone. To make connections to the sample the active cables are sandwiched between two Nb-Ti cables which extend beyond the sample assembly. The Nb-Ti and active cable interleaved with sheets of eutectic Pb-Sn solder. A U-shaped copper box with a copper lid holds the stack together while it is heated. Pressure applied to the lid during heating compresses the stack when the solder melts. This technique produces a robust joint with low resistivity (< 1 nΩ-cm). The same solder box technique was used at the bottom of the sample to join the two active cables forming the current return.

Voltage taps were attached to the sample at four locations. Prior to heat treatment 304 stainless steel strips 0.025 mm thick were wrapped around the cable at the voltage tap locations. These stainless steel taps were in contact with all of the strands of the cable. After heat treatment twisted pair leads are soldered to these stainless steel tabs. Two sets of taps were attached to the active cables between the 122 mm loading section, one on the upper cable and the other on the lower cable. These taps were 170 mm apart. The third pair were attached to the active cables just above the lower solder joint so that its resistivity can be monitored. The fourth pair were attached to the active cables at the two lead solder boxes so that the total voltage of the sample could be monitored.

After all of the solder connections to each cable have been made the sample is assembled in test tooling and potted. During assembly the sample is shimmed to the same theoretical thickness that was used for the heat treatment. The sample and the 304 stainless test tooling are then vacuum impregnated in a vertical orientation with Composite Technology Development 101 (CTD-101) epoxy producing a rugged test assembly.

The test tooling had a specially designed cover plate to permit uniform loading of the cable by the piston. Electrical discharge machine wire cuts along the plate produced a beam whose ends were attached and whose width matched that of the cable such that when loaded it deflects into the sample uniformly regardless of piston alignment.

C. Magnet and Loading System

The NHMFL has a split pair solenoid magnet with the solenoid axis in the horizontal orientation [2]. The magnet was manufactured by Oxford Instruments and can produce a field of 13 T. This permits cables to be tested with the magnetic field perpendicular to the current in the cables. Samples are inserted into a radial access port, 30 mm by 70 mm, which is perpendicular to the solenoid axis. A schematic of the sample assembly in the magnet is shown in Fig. 2. The inside diameter of the solenoid is 150 mm. The loading assembly was designed to fit into this space.

A schematic of the loading assembly with piston, bellows, and housing are shown in Fig. 3. All of the components are made from 304L stainless steel. The radial access port of the piston is reduced to 25 mm by 65 mm. This defined the maximum sample size to about 24.5 mm by 64 mm. The bellows and piston assembly were designed for He gas pressures up to 10 MPa (1,500 psi), which is just below the solidification of liquid helium at 4 K. The reduction in area between the ends of the piston produces a 6 fold increase in pressure. The further reduction in area of the beam in the cover plate permits pressures of 380 MPa to be attained.

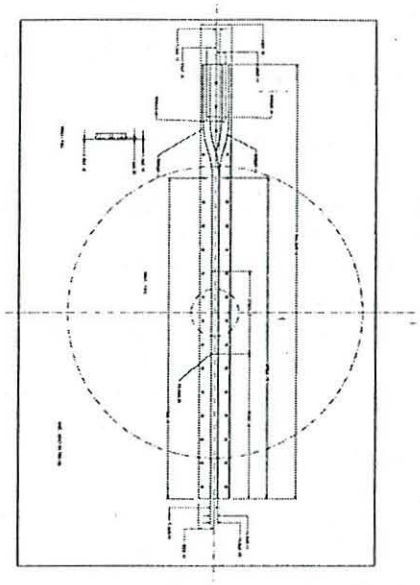

Fig. 2. Schematic of the sample holder superimposed on the magnet. The bore and outside diameter of the magnet are shown as dotted lines in the drawing. The magnet bore is 150 mm. The sample is shown in the testing orientation.

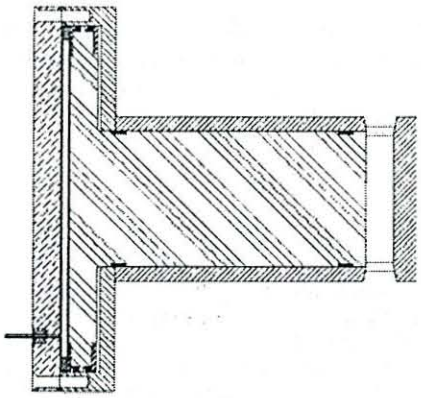

Fig. 3. Bellows, piston, and anvil assembly that is inserted into the bore of the slip pair magnets. The outside diameter of the piston and anvil housing is a little less that the magnet bore of 150 mm.

III. Results and Discussion

The variation of I_c with transverse loading of cable 523 is shown in Fig. 4. All of the I_c data for this cable was obtained from I-V curves with a quench behavior. After several training quenches, about 15, a critical current of 12.5 kA is attained. The critical current of the cable was then measured at loads of 50 MPa and 100 MPa. The critical current was reduced to about 10 kA. After unloading the critical current was once again measured and it was 12.8 kA. The critical current increased slightly with the loading and unloading cycle.

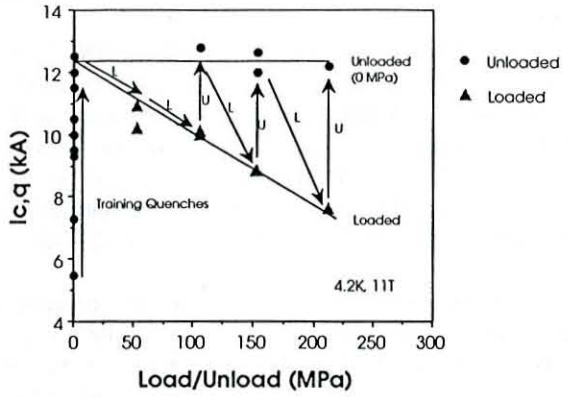

Fig. 4. Critical current (quench) variation with pressure of Nb_3Sn cable 523 used for dipole magnet D20 of LBNL. Cable 523 has 37 strands of internal tin conductor produced by IGC.

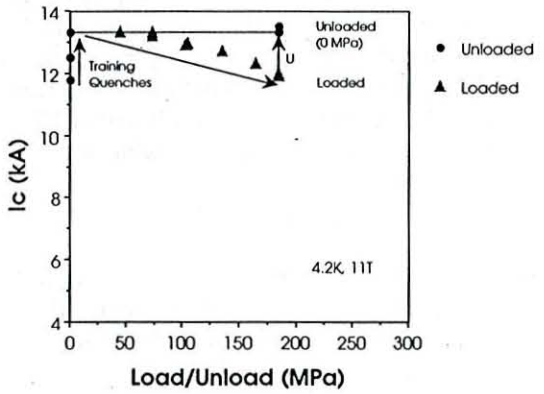

Fig. 5. Critical current variation with pressure of cable 522 used in D20 of LBNL. Cable 523 has 37 strands of modified jelly roll conductor produced by TWC.

The cable was then put through the following loading and unloading sequence: 150 MPa, unloaded, 210 MPa, and unloaded. The critical current was measured at each pressurization step and then unloaded to check for any permanent degradation of the cable. The permanent degradation was about 4% after loading to 210 MPa if the I_c of the unloaded virgin cable is 12.5 kA.

The variation in I_c with transverse loading of cable 522 can be seen in Fig. 5. This cable achieved a short sample I_c of 13.5 kA after only 3 quenches. This behavior is very different that of cable 523. All of the I-V curves had a smooth transition permitting easy determination of I_c using a 10^{-12} Ω-cm criteria. However, the cable short sample is about 10 % below what one would expect from the strand I_c of 405 A. From this strand I_c one would calculate a cable I_c of 15.0 kA. At this time the origin of the lower cable I_c is not known but it is believed to be associated with strand damage from cabling. However, the cable showed no irreversible damage for

stresses up to 185 MPa. Past work has shown that cabling damage of strand would show irreversible I_c degradation for low stresses [3].

Some previous cable measurements on TWC conductor have shown it to be more sensitive to transverse loading. At first one may think that there is an inconsistency in the cable behavior but a direct comparison is difficult. This is due to significant difference in internal structure of the strand in different work and most of the earlier work was performed on keystoned cable with large compactions at the narrow edge [3,4].

The internal structure of each strand after reaction can be seen in Fig. 1. There are a few features to be noticed about the two wires of Figs. 1(a) and 1(b). One is the different sub-element geometry and Cu distribution due to the different manufacturing methods. Another is the wire produced by the internal-tin process has much more porosity than that produced by the modified jelly roll process. The authors do not want to get into a discussion of the origin of this porosity but just want to note the differences between the two strands.

Prior work suggests a functional form for the I_c versus pressure behavior for Nb_3Sn [4]. Briefly summarizing the approach, by using the empirical relations for $J_c(T)$ and $J_c(B)$ developed by [4] and using expressions $B_{c2}(\sigma)$ and T_c one can express the change of critical current with pressure in the form:

$$I_c = I_{c0} + I_{c1}P + I_{c2}P^2. \qquad (1)$$

Where P is the traverse pressure on the cable and I_{c0}, I_{c1} and I_{c2} are coefficients determined by fitting the data or theory. By using either relations by Ekin [7] for $B_{c2}(\varepsilon)$ and $T_c(\varepsilon)$ with ε replaced by (σ/E) or ones with a linear form for $B_{c2}(P)$ and $T_c(P)$ by saving only terms in to second order expression (1) is obtained. By substituting values T_{c0}=18.3, Bc2=25T, dT_c/dP= -0.18K/Gpa, and dB_{c2}/dP=-1.2T/G from [8] one can obtain theoretical values for the coefficients. Different values for these coefficients are obtained depending on the empirical expressions used to calculate them and thus give (1) either a linear or quadratic character. Ekin's relations B_{c2} and T_c give a linear form to (1) while linear expressions for B_{c2} and T_c give a quadratic form.

For the cables studied here 523 would have an I_{c1} much greater than I_{c2} while 523 would have I_{c2} much greater than I_{c1}. Prior work to explain the behavior in I_c of cables with transverse pressure has shown that either behavior is possible in Nb_3Sn cable. If one fits the I_c versus loading data for both cables the coefficients for (1) can be obtained and are given in Table III. This shows that the data for 522 is almost quadratic while that of 523 is almost linear.

TABLE III.

Cable No.	Fit	I_{c0} (kA)	I_{c1} (kA/MPa)	I_{c2} (kA/MPa^2)	R^2
522	Quadratic	13.30	2.37×10^{-3}	-5.20×10^{-5}	0.992
522	Linear	13.57	-7.57×10^{-3}	----------	0.871
523	Quadratic	12.13	-1.96×10^{-2}	-9.05×10^{-6}	0.977
523	Linear	12.15	-2.14×10^{-2}	----------	0.977

IV. Conclusions

The results presented here show that two cables one made with IGC strand and the other with TWC strand have very different I_c versus pressure behavior. The critical current of cable 523 made by the internal-tin process (IGC) shows a linear decrease with pressure while the critical current of cable 522 made by the modified jelly roll process is parabolic. The internal tin strand also seems be more sensitive to pressure with a decrease of about 40 % in I_c for loads of 210 MPa. The I_c of the modified jelly roll strand (TWC) only decrease by 11 % at a pressure of 185 MPa. It may be premature to made strong statements as to the origin of these differences in behavior but the different internal structure of the two strands suggest that the high porosity of internal tin strand is detrimental.

Acknowledgment

The authors would like to thank the technical staff of the NHMFL for all of their assistance during experimental set up and testing. DRD would like to thank Andy Powell and Peter Murphy of NHMFL's electronic support group for equipment fabrication and system diagnostics.

References

[1] A. D. McInturff, R. Benjegerdes, P. Bish, S. Caspi, K. Chow, D. Dell'Orco, D. R. Dietderich, R. Hannaford, W. Harnden, H. Higley, A. Lietzke, L. Morrison, M. Morrison, R. Scanlan, J. Smithwick, C. Taylor, and J. van Oort, "Test results for a high field (13T) Nb_3Sn dipole," Proc. Particle Accel. Conf., May 12-16, Vancouver, B.C. Canada., in press.

[2] L.T. Summers, R. P. Walsh, and J. R. Miller, "A facility for the characterization of the critical current of superconductors as a function of strain and magnetic field," IEEE Trans. Appl. Super., vol. 5 pp. 1896-1899, June 1995.

[3] J. M. van Oort, R. M. Scanlan, H.W. Weijers, S. Wessel, H.H.J. ten Kate, "The reduction of the critical current in Nb_3Sn cables under transverse loads," IEEE Trans. Appl. Super., vol. 3 pp. 559-562, March 1993.

[4] J. M. van Oort, Ph. D. Thesis in progress, University of Twente, Netherlands.

[5]. H.H.J. ten Kate, H.W. Weijers, J.M. van Oort, "Critical current degradation in Nb_3Sn cables under transverse pressure," IEEE Trans. Appl. Super., vol. 3 pp. 1334-1337, March 1993.

[6] D.P. Hampshire, H. Jones, and E.W.J. Mitchell, "An in-depth characterization of (Nb,Ta)3Sn filamentary superconductor,' IEEE Trans. Mag., Vol. MAG-21, pp. 289-292, March1985

[7] J.W. Ekin, "Strain scaling law for flux pinning in practical superconductors. Part1: Basic relationships and application to Nb3Sn conductors," Cryogenics, vol. 20, p 611, 1980.

[8] B. ten Haken, "Strain effects on the critical properties of high-field superconductors," Ph. D. Thesis, University of Twente, Netherlands. September 1994.